cmgh
CELLULAR AND MOLECULAR GASTROENTEROLOGY AND HEPATOLOGY

ORIGINAL RESEARCH

The Microbiome Activates CD4 T-cell–mediated Immunity to Compensate for Increased Intestinal Permeability

Karen L. Edelblum,[1,2] Gil Sharon,[3] Gurminder Singh,[2,4] Matthew A. Odenwald,[2] Anne Sailer,[2] Severine Cao,[2] Sarina Ravens,[5] Irene Thomsen,[5] Kamal El Bissati,[6,7] Rima McLeod,[6,7] Chen Dong,[8] Sandeep Gurbuxani,[2] Immo Prinz,[5] Sarkis K. Mazmanian,[3] and Jerrold R. Turner[2,4]

[1]*Department of Pathology and Laboratory Medicine, Rutgers New Jersey Medical School, Newark, New Jersey;* [2]*Departments of Pathology,* [6]*Ophthalmology and Visual Sciences, and* [7]*Pediatrics, University of Chicago, Chicago, Illinois;* [3]*Division of Biology and Biological Engineering, California Institute of Technology, Pasadena, California;* [5]*Institute of Immunology, Hannover Medical School, Hannover, Germany;* [8]*Institute for Immunology, Tsinghua University, Beijing, China; and* [4]*Departments of Pathology and Medicine, Brigham and Women's Hospital, Harvard Medical School, Boston, Massachusetts*

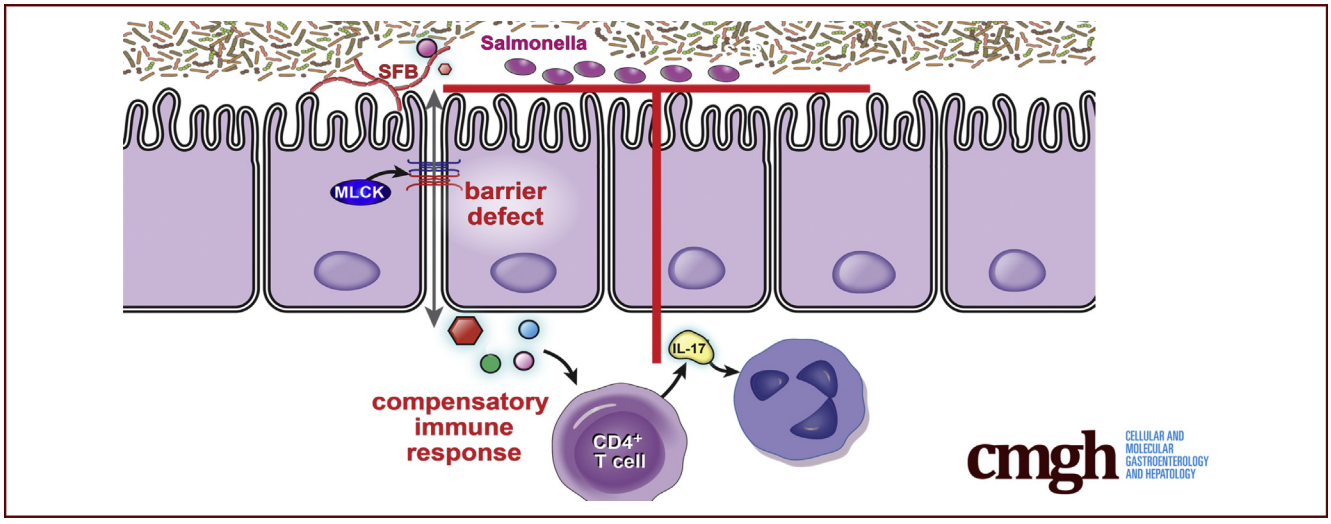

SUMMARY

Despite common perceptions, studies of human subjects and experimental animals show that intestinal barrier loss is insufficient to induce disease in healthy individuals. Here we define a compensatory immune response that prevents pathogen invasion in mice with chronic barrier loss.

BACKGROUND & AIMS: Despite a prominent association, chronic intestinal barrier loss is insufficient to induce disease in human subjects or experimental animals. We hypothesized that compensatory mucosal immune activation might protect individuals with increased intestinal permeability from disease. We used a model in which intestinal barrier loss is triggered by intestinal epithelial-specific expression of constitutively active myosin light chain kinase (CA-MLCK). Here we asked whether constitutive tight junction barrier loss impacts susceptibility to enteric pathogens.

METHODS: Acute or chronic *Toxoplasma gondii* or *Salmonella typhimurium* infection was assessed in CA-MLCK transgenic or wild-type mice. Germ-free mice or those lacking specific immune cell populations were used to investigate the effect of microbial-activated immunity on pathogen translocation in the context of increased intestinal permeability.

RESULTS: Acute *T gondii* and *S typhimurium* translocation across the epithelial barrier was reduced in CA-MLCK mice. This protection was due to enhanced mucosal immune activation that required $CD4^+$ T cells and interleukin 17A but not immunoglobulin A. The protective mucosal immune activation in CA-MLCK mice depended on segmented filamentous bacteria (SFB), because protection against early *S typhimurium* invasion was lost in germ-free CA-MLCK mice but could be restored by conventionalization with SFB-containing, not SFB-deficient, microbiota. In contrast, chronic *S typhimurium* infection was more severe in CA-MLCK mice, suggesting that despite activation of protective mucosal immunity, barrier defects ultimately result in enhanced disease progression.

CONCLUSIONS: Increased epithelial tight junction permeability synergizes with commensal bacteria to promote intestinal $CD4^+$ T-cell expansion and interleukin 17A production that limits

enteric pathogen invasion. *(Cell Mol Gastroenterol Hepatol 2017;4:285–297; http://dx.doi.org/10.1016/j.jcmgh.2017.06.001)*

Keywords: Barrier Function; Tight Junction; Microbiota; CD4 T Cell; Mucosal Immunity; Salmonella.

The intestinal epithelium supports nutrient absorption and secretion but also serves as a selectively permeable barrier that separates the mucosal immune system from the intestinal lumen.[1–3] The association of many inflammatory bowel disease risk alleles with mucosal immunity and bacterial recognition[4] suggests that intact epithelial barrier, which limits microbial contact with the immune system, may prevent a severe inflammatory response in susceptible individuals. Consistent with this idea, intestinal barrier function is compromised in Crohn's disease and has been identified as a marker of impending disease reactivation.[5,6] Nevertheless, modest barrier loss is present in a subset of healthy first-degree relatives of Crohn's disease patients and has been associated with specific polymorphisms of the muramyl dipeptide receptor NOD2.[7,8] These human data correlate with results from rodent models showing that epithelial barrier dysfunction alone is not sufficient to initiate disease.[9–11]

The mechanisms that prevent disease in individuals with increased intestinal permeability are poorly understood. Although mouse models can be useful in dissecting these processes, most display far greater intestinal permeability increases than those seen in healthy individuals with modest barrier loss[7,12,13] and use mechanisms that may not be relevant to human disease. We have focused on myosin light chain kinase, which is well-recognized as a physiologically and pathophysiologically relevant regulator of tight junctions and the intestinal barrier.[3,14] Transgenic mice that express constitutively active myosin light chain kinase (CA-MLCK)[14–16] within the intestinal epithelium exhibit targeted increases in intestinal tight junction permeability,[9] but, unlike most other rodent models, they do not display evidence of epithelial damage such as increased epithelial proliferation and migration.[9–11] Therefore, CA-MLCK mice provide an exquisitely targeted model of increased intestinal tight junction permeability that is not associated with epithelial damage but is quantitatively and qualitatively similar to barrier defects observed in healthy Crohn's disease relatives.

It is now widely recognized that the intestinal microbiota shape mucosal immunity through mechanisms including stimulation of innate immune cells by commensal-derived products and induction of T-cell polarization.[17,18] These data indicate the presence of a continuous feedback loop in which commensal bacteria "instruct" host immunity to induce tolerance to the local microenvironment or, alternatively, serve as a rheostat to modulate pathogen clearance or autoimmunity. In addition to the epithelial barrier, several mechanisms have evolved to limit pathogen invasion,[19] including the synthesis of antimicrobial immunoglobulin (Ig) A and IgG by plasma cells in the lamina propria (LP) that is in turn transported across the epithelium into the intestinal lumen.[20]

Increased intestinal permeability is not sufficient to promote spontaneous disease.[9–11,21,22] However, constitutive barrier loss in CA-MLCK mice does induce subclinical immune activation and increased susceptibility to experimental immune-mediated colitis.[9] Notably, the barrier loss in these mice is due to selective effects on tight junction permeability and is insufficient to trigger epithelial damage.[9,23] We hypothesized that the barrier defects resulting from CA-MLCK expression would render these mice more susceptible to enteric infection.

Surprisingly, our data show that CA-MLCK mice are protected against early pathogen invasion. This protection depended on adaptive immunity via LP $CD4^+$ T-cell expansion, interleukin 17A (IL17A) production, and enhanced neutrophil recruitment in infected CA-MLCK mice relative to infected wild-type (WT) mice. Protection was abrogated in germ-free CA-MLCK mice, indicating that commensal microbes promote a mild Th17 response that limits early pathogen translocation. Although increased tight junction permeability protected against acute bacterial invasion, CA-MLCK mice did develop more severe intestinal and systemic disease during chronic infection. These data provide new insight into the mechanisms that mucosal immunity adapts to physiological-range epithelial barrier defects and how this compensation eventually fails in the context of chronic inflammatory disease.

Materials and Methods

Animals

Mice were 8–12 weeks of age, maintained on a C57BL/6 background, and housed under specific pathogen–free (SPF) conditions. WT, *Rag1* KO, and *Tcrd* KO mice were obtained from the Jackson Laboratories, Bar Harbor, ME. In our colony, all mice were colonized with segmented filamentous bacteria (SFB). CA-MLCK mice[9] were crossed to TcrdH2BeGFP (TcrdEGFP),[24] *IL17A* KO,[25] or *IghA* KO[26] mice (provided by Dennis Metzger, Albany Medical College, Albany, NY).

Germ-free (GF) transgenic CA-MLCK mice were produced by rederivation of SPF C57BL/6J females mated with SPF CA-MLCK males. Briefly, uteri from donor mothers were removed on E19.5 by cesarean section and transferred into a GF isolator in aseptic Virkon solution (DuPont, Parlin, NJ). Offspring were then extracted from the uterus and reared by a GF foster Swiss-Webster mother. Healthy offspring were genotyped, and males harboring the transgene were subsequently used for breeding with GF C57BL/6J females.

Abbreviations used in this paper: **CA-MLCK, constitutively active myosin light chain kinase; CFU, colony-forming unit; GF, germ-free; Ig, immunoglobulin; IL, interleukin; LP, lamina propria; SEM, standard error of the mean; SFB, segmented filamentous bacteria; SPF, specific pathogen–free; WT, wild-type.**

Most current article

2352-345X
http://dx.doi.org/10.1016/j.jcmgh.2017.06.001

For colonization experiments, littermate WT and CA-MLCK mice were removed from the GF isolator at 3–4 weeks of age and gavaged with 100 μL cecal contents from C57BL/6NTac (Taconic Farms, Hudson, NY) or C57BL/6J mice (Jackson Laboratories). Cecal contents were resuspended in sodium bicarbonate solution under anaerobic conditions (1:2 v/v). *Salmonella typhimurium* exposure and tissue sampling were performed 4 weeks after colonization on age-matched GF and conventionalized mice. All studies were conducted in an Association of the Assessment and Accreditation of Laboratory Animal Care (AALAC)–accredited facility according to protocols approved by Rutgers New Jersey Medical School, the University of Chicago, and the California Institute of Technology Institutional Animal Care and Use Committees.

Pathogen Infection

DsRed-labeled *S typhimurium* strain SL3201 were provided by Andrew Neish, Emory University, Atlanta, GA. Mice were anesthetized by intraperitoneal injection of ketamine/xylazine, a 3- to 4-cm loop of jejunum or ileum was exposed, and the luminal surface of the intestine was exposed as described previously.[27] For 30 minutes 10^8 colony-forming units (CFUs) DsRed-SL3201 were applied directly to the exposed luminal surface, after which mice were killed, and the loop of intestine was fixed for analysis by fluorescence microscopy as previously described.[28]

Systemic infection of *S typhimurium* was assessed by oral gavage with 10^8 CFUs DsRed-SL3201 after 24 hours of pretreatment with 100 mg/mL streptomycin. Mice were killed 9 days after infection on the basis of the severity of clinical scores or if an individual mouse lost more than 20% of its initial body weight. Organs were harvested and either fixed in 10% neutral buffered formalin or embedded in optimal cutting temperature (OCT; Sakura, Torrance, CA) medium for further immunohistochemical analysis. Clinical scores were determined on the basis of fur texture, posture, and activity on a scale of 0–2 each, with a potential combined score of 6. Histologic scores of colitis were determined on a scale of 0–2 on the basis of the following criteria: crypt dilation and elongation, presence of crypt abscesses, extent of epithelial erosion, and regeneration as well as the number of apoptotic cells and goblet cells, with a potential combined score of 14. Histologic scores of the spleen were determined on a scale of 0–3 on the basis of the immune cell infiltrate and the presence of neutrophils.

The ME49 strain of *Toxoplasma gondii* was maintained as tachyzoites by serial passage in human foreskin fibroblasts as previously described.[29] The 10- to 12-week-old female HLA-B*0702 transgenic mice[29] were infected intraperitoneally with 1×10^4 ME49 type II tachyzoites. Tissue cysts were isolated from the brains of these mice 22 days after infection and quantified.[30] Mice were gavaged with 10 cysts in 100 μL sterile phosphate-buffered saline and killed after 1 hour to assess parasite translocation.

Immunofluorescence and Image Analysis

Mouse intestine was fixed in 1% paraformaldehyde for 2 hours, washed with 50 mmol/L NH_4Cl, and cryoprotected in 30% sucrose (w/v) at 4°C overnight. Tissue was then embedded in OCT medium, snap-frozen, and stored at −80°C. Alternatively, cryosections of tissue that was snap-frozen without prior fixation were fixed in 1:1 methanol:acetone for 10 minutes at −20°C. Frozen sections were immunostained as previously described[31] by using primary antibodies, rabbit anti-myeloperoxidase, rabbit anti-CD3 (Abcam, Cambridge, MA), rabbit anti-LDH1 antiserum,[32] rat anti-CD4, rat anti-IgA (BD Pharmingen, San Jose, CA), followed by AlexaFluor-conjugated phalloidin or secondary antibodies and Hoechst 33342 dye (Invitrogen, Carlsbad, CA). Slides were mounted with Prolong Gold (Invitrogen) and visualized on a DMI6000 inverted epifluorescence microscope equipped with a Rolera EMC2 CCD camera (QImaging, Surrey, BC, Canada), ×20/0.50 PH2, ×40/0.60CORR/PH, or ×63/0.70CORR objectives, and Metamorph 7 acquisition software (Molecular Devices, Sunnyvale, CA). Four μm Z-stacks were acquired with 0.2 μm spacing, and images were deconvolved for 10 iterations by using Autodeblur (Media Cybernetics, Rockville, MD).

Morphometric analysis of *S typhimurium* and *T gondii* was quantified as previously described.[28] Briefly, invasion was quantified as the number of organisms that had invaded into an epithelial cell or crossed into the LP. Epithelial invasion required the organism to be localized basal to the perijunctional actomyosin ring, as defined by phalloidin staining. Unprocessed images were used for quantitative analyses to avoid potential deconvolution artifact. For each mouse, 6–8 fields, each containing approximately 0.1 mm^2 of epithelial-covered villus mucosa, were analyzed by a blinded observer.

Intestinal Permeability

Mice were fasted for 3 hours and then gavaged with 1 mg/mL fluorescein and 20 mg/mL 70 kDa rhodamine dextran in water. Blood was collected 3 hours later via the retro-orbital sinus. Fluorescence intensity was determined by using a plate reader at 495 nm excitation/525 nm emission and 555 nm excitation/585 nm emission. Intestinal permeability was reported as serum fluorescein recovery normalized to that of 70 kDa rhodamine dextran, which cannot cross tight junctions.

CD4 Depletion and Adoptive Transfer

$CD4^+$ T cells were depleted by injecting mice intraperitoneally with 0.2 mg GK1.5 (University of Chicago Monoclonal Antibody Core). Injection of 0.2 mg IgG isotype control (F156-6B9.7) was used as a control. $CD4^+$ T-cell depletion was confirmed after 48 hours by either flow cytometric analysis of retro-orbital blood (before infection) or splenocytes (on death).

Eight-week-old *Rag1* KO or *Rag1* KO CA-MLCK mice were injected with 2×10^6 $CD4^+$ splenocytes from sex-matched 10-week-old C57BL/6 donor mice. $CD4^+$ T cells were enriched by negative selection (Miltenyi Biotech, San Diego, CA), sorted to 98% purity by flow cytometry, and injected retro-orbitally. Infections were performed 2 weeks after adoptive transfer. Age-matched mice not receiving adoptive transfer were used as controls.

Immunoglobulin A Enzyme-linked Immunosorbent Assay

Fecal samples were homogenized in 0.01% NaN_3 in phosphate-buffered saline and centrifuged, and the supernatant was used for analysis. Plates were coated with 2 μg/mL goat anti-mouse IgA (Southern Biotech, Birmingham, AL) in phosphate-buffered saline, and samples were diluted in 1% bovine serum albumin and incubated overnight at 4°C. Mouse IgA (clone M18-254; BD Pharmingen, San Diego, CA) was used to generate a standard curve. After washes in phosphate-buffered saline containing 0.05% Tween, anti-IgA-avidin phosphatase (Southern Biotech) was added, and *p*-nitrophenyl phosphate was used to develop the reaction. Samples were read by plate reader at 405 nm.

Immunoglobulin A Repertoire Analysis

454 sequencing. After RNA extraction from fecal pellets, cDNA synthesis was performed with SuperScript III (Invitrogen) by using random hexamer primer. Template libraries of rearranged IgA sequences were generated by polymerase chain reaction using a primer specific for the constant Ca (IgA) region (5′CGTATCGCCTCCCTCGCGCCATCAG(MID)GAGCTCGTGGAGTGTCAGTG-3′) and a primer binding at all Vh genes (5′-CTATGCGCCTTGCCAGCCCGCTCAGGAGGTGCAGCTGCAGGAGTCTGG-3′).[33,34] MIDs of 4-nucleotides at constant Ca/Cμ primers allowed to pool samples within sequencing lanes. Following polymerase chain reaction conditions were used: 95°C, 4 minutes; ×25 (94°C, 30 seconds; 62°C, 30 seconds; 72°C, 35 seconds); and 72°C for 10 minutes. Amplicons were purified by Qiaquick Gel Extraction kit (Qiagen, Germantown, MD) and prepared for 454 sequencing using the GS FLX Titanium SV emPCR Lib-A kit and Genome Sequencer FLX system as recommended by the manufacturer.

Sequence analysis. Sequences were annotated and compared with reference sequences of the ImMunoGeneTics (IMGT) HighV-QUEST database.[35,36] IMGT results were sorted for productive sequences and further analyzed with Excel and VBA (Microsoft Corp, Redmond, WA).[33] To compare between samples we randomly analyzed 5000 CDR3 sequences per sample. The Shannon index is used to measure IgA repertoire diversity and was calculated with R studio (version 0.94.110; http://www.r-project.org/, http://rstudio.org/) and the library "vegan" (command: diversity). For quantification of VDJ segment usage only major chains were taken into consideration.

Statistical Analysis

All data are presented as either the mean ± standard error of the mean (SEM) or with a 95% confidence interval. *P* values of direct comparisons between 2 independent samples were determined by a two-tailed Student *t* test and considered to be significant if $P \leq .05$. Mann-Whitney rank sum tests were performed in cases in which the data were not normally distributed. Comparisons between multiple independent variables were determined by one-way analysis of variance, and Holm-Sidak method was used for pairwise comparisons. In instances in which the data were not normally distributed, Kruskal-Wallis one-way analysis of variance on ranks was performed, and the Dunn method was used for multiple pairwise comparisons.

Results

Epithelial Constitutively Active Myosin Light Chain Kinase Expression Results in Increased Intestinal Permeability

The epithelial tight junction is intimately associated with a perijunctional actomyosin ring that modulates paracellular permeability via MLCK. CA-MLCK expression[9,14] within the intestinal epithelium markedly increased perijunctional myosin II regulatory light chain phosphorylation (Figure 1*A*) and also enhanced small intestinal paracellular, ie, tight junction, permeability in a size-selective manner (Figure 1*B*). Despite this barrier defect, CA-MLCK mice did not develop spontaneous colitis. On the basis of these data and the potential link between enteric infection and subsequent development of inflammatory bowel disease,[37,38] we hypothesized that constitutive barrier dysfunction may predispose these animals to enteric infection.

Increased Intestinal Epithelial Permeability Activates Processes That Limit Early Pathogen Translocation

Intestinal permeability, the converse of barrier function, is regulated through paracellular flux. Paracellular transport via the tight junction is size-selective and precisely regulated. In contrast, unrestricted flux, which represents flux across damaged epithelia,[3,39,40] allows passage of large molecules and whole bacteria. CA-MLCK mice exhibit increases in paracellular permeability that are similar to those seen in Crohn's disease patients during remission as well as in a subset of their healthy relatives.[9] Therefore, we

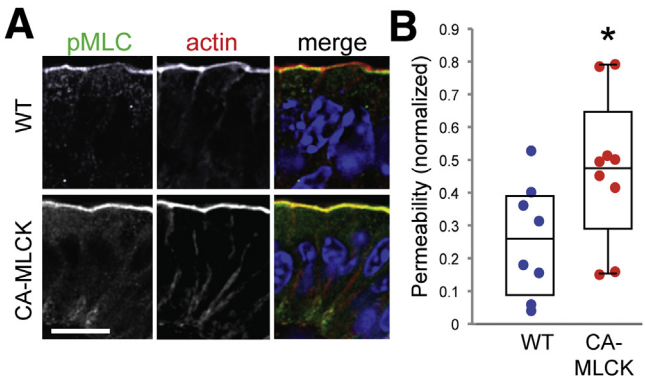

Figure 1. Constitutive epithelial expression of CA-MLCK increases intestinal permeability. (*A*) MLC phosphorylation (*green*) at the epithelial perijunctional actomyosin ring (f-actin, *red*) in WT and CA-MLCK mice. Nuclei are shown in *blue*. Scale bar, 20 μm. (*B*) Small intestinal permeability is shown as ratio of paracellular flux of fluorescein and 70 kDa rhodamine dextran in WT and CA-MLCK mice. n = 8–9 mice per genotype; data from 2 independent experiments are shown. *$P < .05$.

chose this model to investigate the impact of physiologically relevant tight junction barrier defects on host defense.

As previously reported in the colon,[9] LP CD4$^+$ T-cell numbers were increased in the small intestine of CA-MLCK, relative to WT, mice (Figure 2*A* and *B*). To investigate how tight junction barrier loss and the associated LP immune expansion affect susceptibility to enteric pathogens, CA-MLCK and WT mice were infected orally with the intracellular protozoan parasite *T gondii* (Figure 2*C*). Within 1 hour, the number of parasites that had transmigrated across the epithelium and into the LP was reduced by 50% ± 8% in CA-MLCK mice relative to WT (Figure 2*D*). Paradoxically, this indicates that increased intestinal permeability limits parasite invasion. To determine whether this barrier defect also conferred protection against other pathogens, mice were exposed to *S typhimurium.* As with the protozoan, bacterial translocation was reduced by 76% ± 6% in CA-MLCK relative to WT mice (Figure 2*E* and *F*).

To determine whether the increased LP infiltration of adaptive immune cells was required for CA-MLCK–mediated protection against bacterial invasion, *Rag1* knockout (KO); CA-MLCK mice lacking both B and T cells were challenged with *S typhimurium*. Bacterial translocation in *Rag1* KO; CA-MLCK mice was similar to that in *Rag1* KO mice alone (Figure 2*E* and *F*), indicating that adaptive immunity is required for the protective effect of CA-MLCK expression. γδ T cells also contribute significantly to protection from early pathogen invasion.[28,41] This was confirmed in our experiments, which showed greater *S typhimurium* invasion in *Tcrd* KO mice, which lack γδ T cells (Figure 2*E* and *F*).

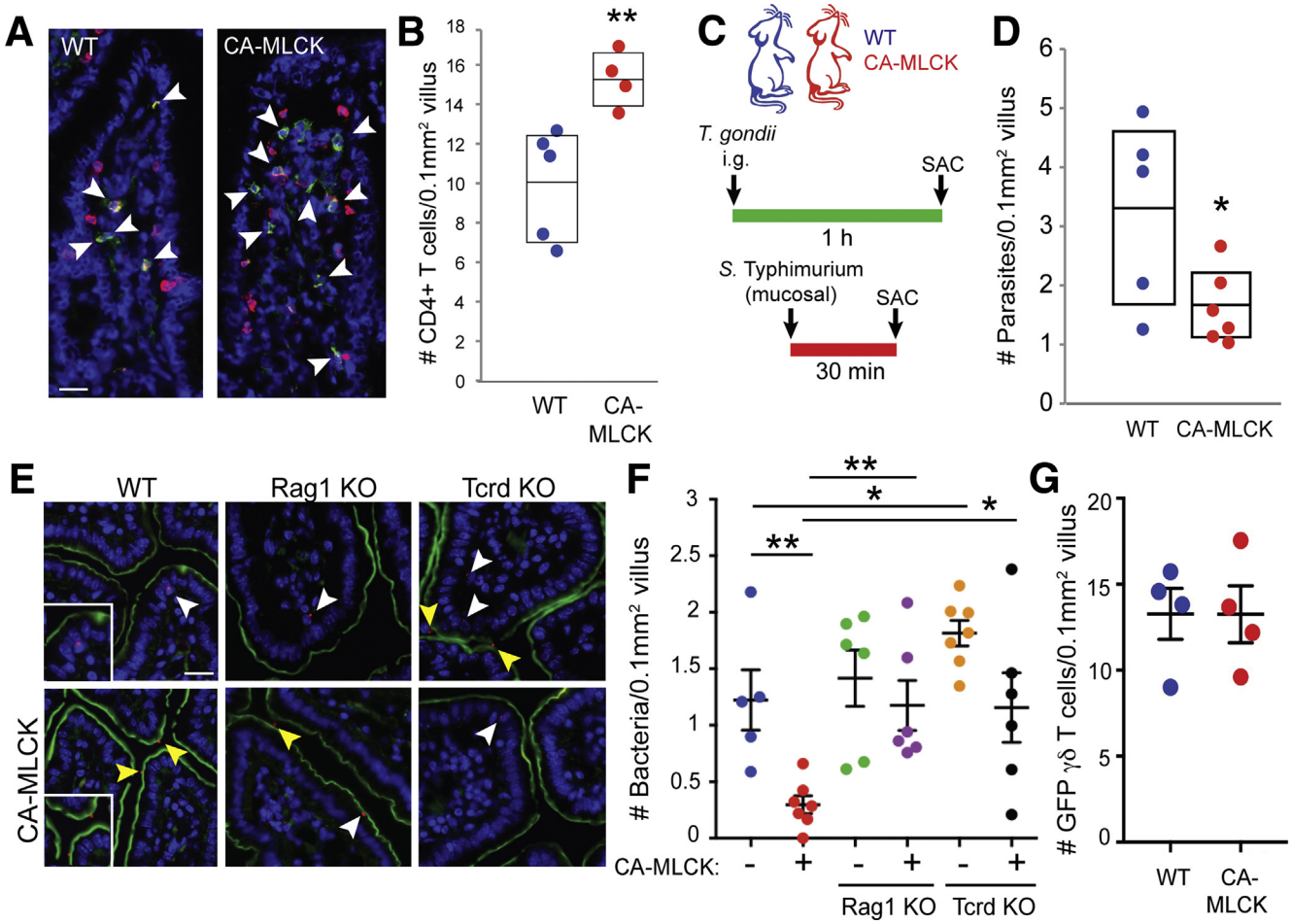

Figure 2. Increased intestinal permeability limits early enteric pathogen invasion. (*A*) Fluorescence micrographs of CD3$^+$ CD4$^+$ LP T cells in WT and CA-MLCK mice. CD3, *red*; CD4, *green*; nuclei, *blue*. *White arrowheads* indicate CD4$^+$ T cells. Scale bar, 20 μm. (*B*) Morphometric analysis of LP CD4$^+$ T cells. n = 4–5 mice. $^{**}P < .01$. (*C*) WT and CA-MLCK mice were orally administered *T gondii* cysts and killed after 1 hour (SAC). Alternatively, mice were exposed to *S typhimurium* through the addition of 10^8 CFUs directly to the mucosal surface for 30 minutes. (*D*) Morphometric analysis of parasite translocation 1 hour after infection. n = 5–6 mice from 2 independent experiments. $^{*}P < .05$. (*E*) Fluorescence micrographs of *S typhimurium* (*red, arrows*)–infected WT and CA-MLCK mice crossed to *Rag1*- or γδ T-cell (*Tcrd*)–deficient backgrounds. Nuclei, *blue*; f-actin, *green*. *White arrowheads* indicate translocation of *S typhimurium*, whereas *yellow arrowheads* are bacteria not counted. Scale bar, 20 μm. (*F*) Morphometric analysis of *S typhimurium* invasion. n = 5–7 mice from at least 2 independent experiments. Approximately 200 villi were counted for each condition. $^{*}P < .05$, $^{**}P < .01$. (*G*) Morphometric analysis of γδ T cells in WT and CA-MLCK mice. n = 4 mice. Mean ± SEM are shown.

However, CA-MLCK expression within *Tcrd* KO mice markedly reduced bacterial invasion, indicating that although important to overall host defense, γδ T cells did not account for the observed effects of CA-MLCK expression (Figure 2*E* and *F*). Consistent with this, γδ T-cell numbers were similar in CA-MLCK and WT mice (Figure 2*G*). Taken together, these data demonstrate that increased epithelial permeability promotes immune activation to markedly reduce early invasion of parasites and bacterial pathogens during the initial stages of infection. This protection requires adaptive immunity but is γδ T-cell–independent.

$CD4^+$ T Cells Are Required for Constitutively Active Myosin Light Chain Kinase–induced Protection Against Bacterial Invasion

To better elucidate the immune cell populations contributing to the invasion-resistant phenotype of CA-MLCK mice, we depleted $CD4^+$ T cells and challenged mice with luminal *S typhimurium* (Figure 3*A* and *B*). $CD4^+$ T-cell depletion had no effect on early bacterial translocation in WT mice but increased bacterial invasion more than 5-fold in CA-MLCK mice, relative to mice receiving control IgG (Figure 3*C*). The disparity between CA-MLCK and WT mice suggests that our initial hypothesis that increased tight junction permeability would enhance pathogen invasion was correct. However, the data also indicate that constitutive barrier dysfunction also elicits a $CD4^+$ T-cell response that confers protection against acute pathogen invasion.

The data above indicate that $CD4^+$ T cells are necessary for the protection observed in CA-MLCK mice. To determine whether these cells were sufficient to confer protection, WT $CD4^+$ T cells were adoptively transferred into *Rag1* KO or *Rag1* KO; CA-MLCK recipients (Figure 3*D*). Within 2 weeks, $CD4^+$ T cells were effectively reconstituted in the LP of both CA-MLCK and WT mice (Figure 3*E*). Notably, 73% more LP $CD4^+$ T cells were present in the LP of *Rag1* KO; CA-MLCK, relative to *Rag1* KO, recipients (Figure 3*E*). Whereas $CD4^+$ T-cell transfer into *Rag1* KO mice had no effect on bacterial invasion, $CD4^+$ T-cell transfer into *Rag1* KO; CA-MLCK mice reduced invasion by 43% (Figure 3*F*). These data demonstrate that $CD4^+$ T cells are sufficient to limit early *S typhimurium* invasion. Because $CD4^+$ T cells from WT mice were protective in *Rag1* KO; CA-MLCK mice, the data indicate that changes in the local mucosal

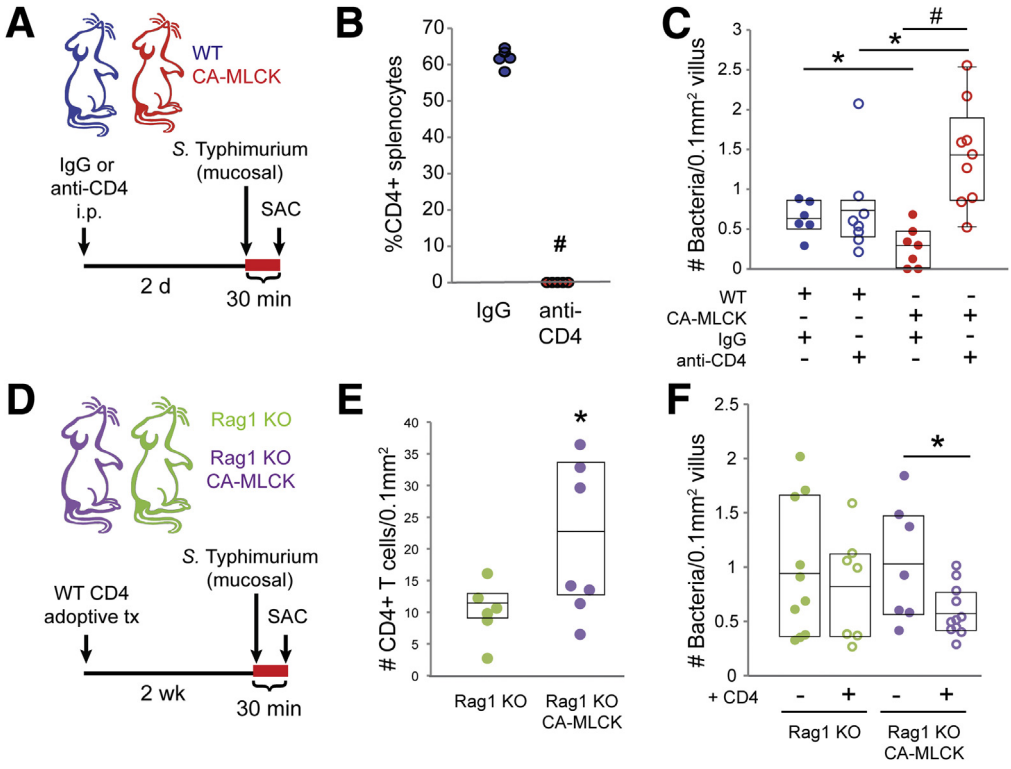

Figure 3. $CD4^+$ T cells are required to confer protection against bacterial invasion in CA-MLCK mice. (*A*) After administration of anti-CD4 (GK1.5) or control IgG intraperitoneally, WT and CA-MLCK mice were exposed to *S typhimurium* through direct application of bacteria to small intestinal mucosal surface for 30 minutes and then killed (SAC). (*B*) Percentage of $CD3^+$ $CD4^+$ T splenocytes 48 hours after anti-CD4 administration. $^{\#}P < .001$. (*C*) Morphometric analysis of *S typhimurium* invasion after administration of anti-CD4 or control IgG. n = 6–9 mice from 2 independent experiments. $^{*}P < .05$, $^{\#}P < .001$. (*D*) *Rag1* KO mice and those also expressing the CA-MLCK Tg received $CD4^+$ T-cell adoptive transfer. After 2 weeks of engraftment, mice were exposed to *S typhimurium* for 30 minutes. (*E*) Morphometric analysis of $CD4^+$ LP T cells in *Rag1* KO and *Rag1* KO CA-MLCK mice after $CD4^+$ T-cell adoptive transfer. n = 7–8 mice from 2 independent experiments. $^{*}P < .05$. (*F*) Analysis of *S typhimurium* translocation in *Rag1* KO and *Rag1* KO; CA-MLCK mice receiving $CD4^+$ T-cell adoptive transfer. n = 7–11 mice from 2 independent experiments. $^{*}P < .05$.

microenvironment resulting from constitutive barrier loss are sufficient to impart this phenotype. This may reflect expansion or enhanced recruitment of $CD4^+$ T cells to the LP of *Rag1* KO; CA-MLCK mice. In either case, it is clear that the compensatory response to epithelial barrier loss includes promotion of a new $CD4^+$ T-cell function that is not otherwise present, as indicated by the failure of $CD4^+$ T cells to reduce bacterial invasion in *Rag1* KO mice.

We also asked whether other components of adaptive immunity might contribute to the protective phenotype observed in CA-MLCK mice. Plasma cell production of commensal-specific IgA interferes with commensal antigen expression and promotes immune exclusion by limiting bacterial association with the mucosal surface, and this has been implicated in the mucosal immune response to loss of JAM-A expression.[22] Morphometric analysis showed that CA-MLCK mice exhibited an increase in IgA^+ plasma cells within the LP compared with WT (Figure 4*A*). However, there were no differences in mucosal transforming growth factor beta transcripts, expression or localization of the polymeric Ig receptor (*pIgR*), or the amount of secreted (luminal) IgA between CA-MLCK and WT mice (Figure 4*B*).[9]

Despite the lack of quantitative increases in luminal IgA, we hypothesized that increased exposure to bacterial products as a result of enhanced paracellular permeability could promote expansion of plasma cells expressing microbe-specific IgA. To test this, complementary determining region 3 region sequences were analyzed from productive IgA VDJ rearrangements. Although the values indicate a highly diverse IgA repertoire in all samples (Figure 4*C*), no differences were observed between WT and CA-MLCK mice. Furthermore, analysis of the frequency of somatic hypermutations within IgA-producing plasma cells during affinity maturation also failed to identify significant differences between the CA-MLCK and WT mice (Figure 4*D*). Therefore, barrier loss does not affect the quality of mucosal IgA.

Previous studies have linked barrier loss to IgA production. Therefore, we asked whether, despite the negative data above, increases in LP IgA-producing plasma cells could contribute to protection against early pathogen invasion. CA-MLCK mice were bred onto an IgA-deficient

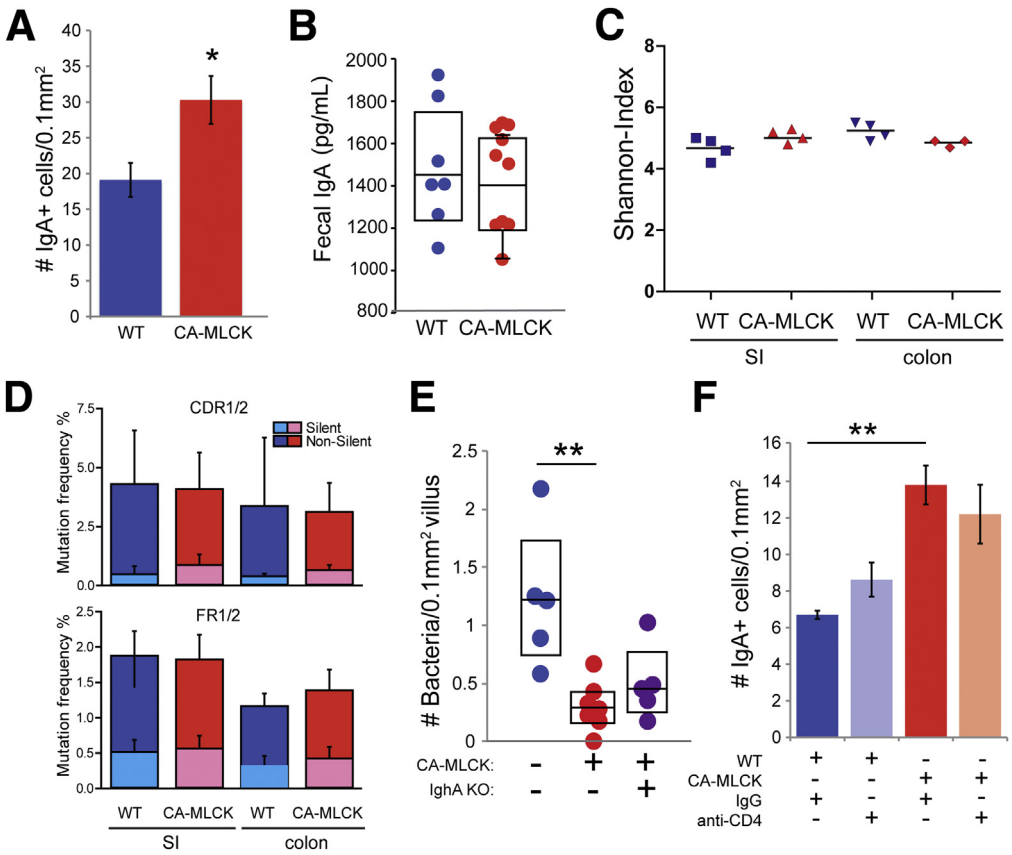

Figure 4. IgA^+ plasma cell number is increased, yet not required for CA-MLCK–mediated protection against bacterial translocation. (*A*) Morphometric analysis of IgA^+ plasma cells in the LP. n = 4–6 mice. Mean ± SEM, $^*P = .05$. (*B*) Enzyme-linked immunosorbent assay for fecal IgA. n = 7–10 mice. Mean ± SEM. (*C*) Shannon Index was calculated from CDR3 sequence pools of given samples. The mean is shown. (*D*) Mutation frequencies in CDR1/2 and FR sequences calculated from the average number of SHM within the Vh region. Frequencies were calculated through division of mutation numbers by the number of nucleotides within the given FR or CDR regions. Mean ± standard deviation. (*E*) Morphometric analysis of *S typhimurium* invasion in WT and CA-MLCK mice on an IghA KO background. n = 5–7 mice from 2 independent experiments. Mean is shown, $^*P = .05$. (*F*) Morphometric analysis of LP IgA^+ plasma cells 48 hours after administration of anti-CD4 or control IgG. Mean ± SEM, $^{**}P < .01$. IghA, immunoglobulin A; SHM, somatic hypermutations.

background (*IghA* KO). Bacterial invasion was similar to CA-MLCK mice regardless of IgA expression (Figure 4*E*), indicating that IgA was not required for the CA-MLCK–mediated protective effect. Because IgA is generated through both T-cell–dependent and –independent mechanisms,[42] we assessed the role of $CD4^+$ T cells in generating increased numbers of LP IgA^+ plasma cells in CA-MLCK mice. $CD4^+$ T-cell depletion did not affect IgA-producing plasma cell number in the LP of CA-MLCK or WT mice (Figure 4*F*). Because of the requirement for $CD4^+$ T cells in the enhanced immunity of CA-MLCK mice, these data lend further support to the conclusion that IgA is not required for the protection observed in CA-MLCK mice.

Interleukin 17A Expression Promotes Neutrophil Recruitment to Prevent Early Bacterial Invasion in Constitutively Active Myosin Light Chain Kinase Mice

Certain strains of commensal bacteria modulate specific immune responses. For example, SFB are known to promote Th17 differentiation in the small intestine,[18,43] and activation of these Th17 cells is critical to pathogen clearance and maintenance of host defense.[44,45] To determine the role of IL17 in $CD4^+$ T-cell–mediated protection against bacterial invasion, CA-MLCK mice were generated on an IL17A-deficient background. IL17A deficiency significantly increased acute *S typhimurium* invasion in CA-MLCK transgenic mice (Figure 5*A*). More strikingly, IL17A knockout eliminated $CD4^+$ T-cell expansion within the LP of CA-MLCK mice (Figure 5*B*). These data show that IL17A is required to generate the increased numbers of LP $CD4^+$ T cells seen in CA-MLCK mice and that both IL17A and $CD4^+$ T cells are necessary for early protection against *S typhimurium* translocation.

One mechanism by which Th17 cells contribute to host defense is induction of granulopoiesis and neutrophil recruitment via CXCL1 and CXCL2 to promote bacterial clearance.[46,47] *S typhimurium* exposure induced rapid neutrophil recruitment into the LP of CA-MLCK but not WT mice (Figure 5*C*). This acute recruitment was eliminated in IL17A KO mice, indicating that IL17A may prime innate immunity for immediate response to initial pathogen exposure.

Commensal Bacteria Are Essential for Activation of Host Defense in Response to Intestinal Epithelial Barrier Dysfunction

The mucosal immune system and microbiota regulate one another during differentiation of the immune response.[2] To test the hypothesis that commensal bacteria drive the mucosal $CD4^+$ T-cell expansion that limits early pathogen invasion, CA-MLCK mice were rederived under GF conditions. Consistent with previous reports, GF mice exhibited significantly diminished numbers of LP lymphocytes. Furthermore, LP $CD4^+$ T-cell and IgA^+ plasma cell numbers were similar in GF CA-MLCK and GF WT mice, indicating that the differences induced by CA-MLCK expression in conventional mice are dependent on the microbiota (Figure 6*A* and *B*). When challenged with *S typhimurium*, invasion was similar in GF CA-MLCK and GF WT mice (Figure 6*C*).

SFB are commensal bacteria known to promote Th17 differentiation in the small intestine and, although abundant in C57BL/6NTac mice from Taconic Farms, are undetectable in C57BL/6J from Jackson Laboratories.[48] Previous studies have shown that in addition to driving Th17 differentiation, SFB colonization of C57BL/6J from Jackson Laboratories promotes Th17-dependent neutrophil recruitment[47] similar to that observed here (Figure 5*C*). To compare the effects of SFB-containing and SFB-deficient microbiota, GF CA-MLCK and WT mice were conventionalized with cecal contents from Taconic Farms (TAC) and Jackson Laboratories (JAX) mice. The enhanced resistance to acute bacterial translocation observed in CA-MLCK mice was restored by SFB-containing (TAC) microbiota, but not by SFB-deficient

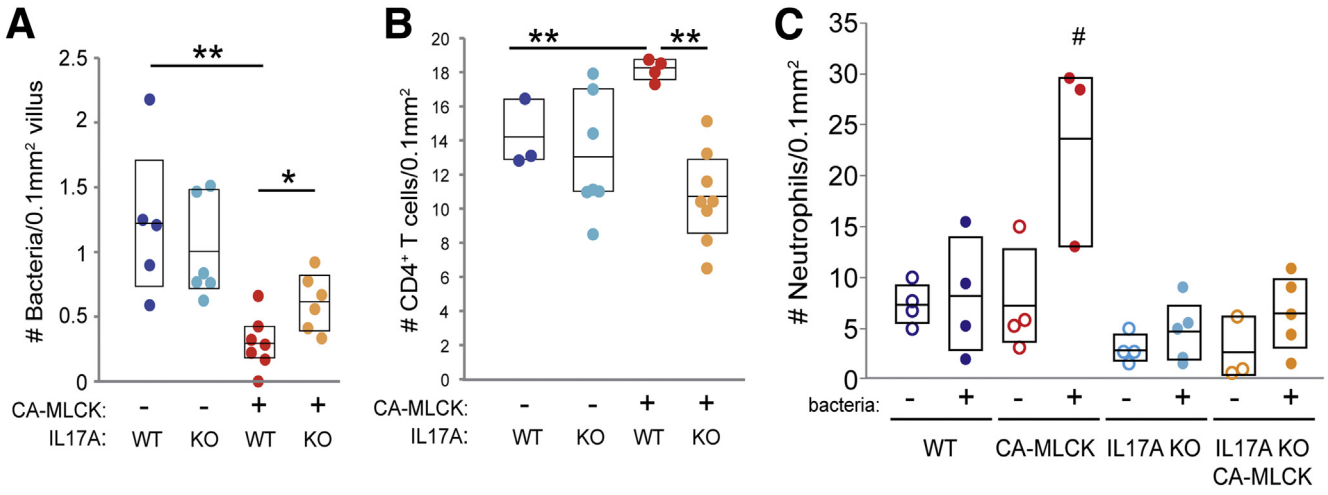

Figure 5. IL17A is required to limit bacterial translocation through promotion of neutrophil recruitment. (*A*) Morphometric analysis of *S typhimurium* invasion in WT and CA-MLCK mice on an IL17A-deficient background. n = 6–7 mice from 2 independent experiments. $^*P < .05$, $^{**}P < .01$. (*B*) Morphometric analysis of $CD4^+$ LP T cells in WT and CA-MLCK mice crossed to IL17A-deficient mice. $^{**}P < .01$. (*C*) Morphometric analysis of neutrophils within the small intestinal LP in uninfected and infected (30 minutes) WT, CA-MLCK, *IL17A* KO or *IL17A* KO; CA-MLCK mice. n = 3–5 mice. $^{\#}P < .001$.

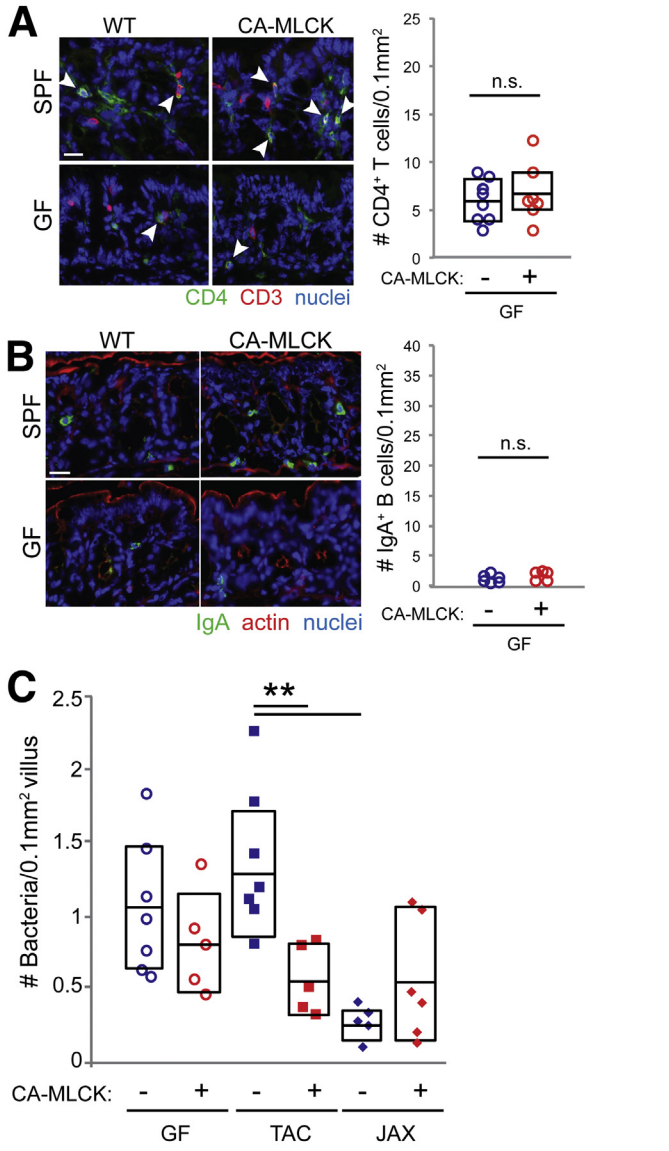

Figure 6. Commensal bacteria are essential for promoting mucosal immune responses to early *Salmonella* invasion in response to increased intestinal permeability. (*A*) Fluorescence micrographs of $CD3^+$ $CD4^+$ LP T cells in WT and CA-MLCK mice raised under either SPF or GF conditions. Scale bar, 20 μm. Morphometric analysis of $CD4^+$ LP T cells in GF WT and CA-MLCK mice are shown. n = 6–8 mice from 2 independent experiments. (*B*) Fluorescence micrographs of IgA^+ plasma cells in the LP in WT and CA-MLCK mice raised under either SPF or GF conditions. Scale bar, 20 μm. Morphometric analysis of IgA^+ plasma cells in GF WT and CA-MLCK mice is shown. n = 5–8 mice from 2 independent experiments. (*C*) Morphometric analysis of *S typhimurium* invasion (30 minutes) in WT and CA-MLCK mice maintained under GF conditions or conventionalized with Taconic (TAC) or Jackson (JAX) microbiota. n = 5–8 mice from 2 independent experiments. $^{**}P < .01$.

(JAX) microbiota (Figure 6*C*). Together with the aforementioned results, these data suggest that SFB-induced Th17 differentiation is central to the protection against acute *S typhimurium* invasion in CA-MLCK mice.

Constitutive Barrier Dysfunction Increases Susceptibility to Chronic Salmonella Infection

The data above demonstrate that tight junction barrier loss results in markedly enhanced pathogen invasion in CD4 T-cell–depleted mice. In immunocompetent mice, tight junction barrier loss also activates mucosal immune responses that limit acute *S typhimurium* invasion. We asked whether these compensatory immune responses were sufficient to prevent chronic infection and systemic salmonellosis. Nine days after infection, CA-MLCK mice exhibited more severe disease, as assessed clinically by reduced activity and hunched posture (Figure 7*A* and *B*), as well as greater mucosal damage and LP lymphoplasmacytic infiltrates (Figure 7*C* and *D*). Differences between CA-MLCK and WT mice were also apparent within the spleen. CA-MLCK mice had sinus thrombi and dense lymphohistiocytic infiltrates that were reminiscent of, but more diffuse than, typhoid nodules, whereas WT mice displayed neutrophil-rich intrasplenic abscesses (Figure 7*E* and *F*). Thus, although increased intestinal epithelial tight junction permeability activates protective immune activation that limits early invasion, this is ultimately insufficient to compensate for barrier loss in the context of chronic disease.

Discussion

Targeted increases in paracellular flux through the epithelial tight junction enhance susceptibility to experimental, immune-mediated colitis.[9] Although tight junction–specific barrier loss is insufficient to allow translocation of intact microbes, we hypothesized that it would increase susceptibility to enteric infection. Our data support this hypothesis in the absence of adaptive immunity but also demonstrate that chronic tight junction barrier loss stimulates a subclinical immune response that limits acute invasion of enteric pathogens. This early protection requires $CD4^+$ T cells and IL17A, but not IgA.

Consistent with previous studies by us and others,[9,21,22] we found that $CD4^+$ LP T-cell number is increased in response to constitutive barrier loss. Notably, the physiologically relevant, tight junction–specific barrier loss studied here is not associated with chronic epithelial damage or homeostatic increases in epithelial proliferation. Furthermore, unlike transient, damage-associated barrier loss,[21] regulatory T-cell populations are not expanded in CA-MLCK mice.[9,21] The increased paracellular permeability resulting from MLCK activation induced an immune response that limited not only early bacterial invasion but also the transmigration of *T gondii.* We found that $CD4^+$ T cells, and in particular Th17 cells, were necessary to limit acute *S typhimurium* invasion in CA-MLCK mice. The data further suggest that IL17A-induced neutrophil recruitment contributes to this enhanced immunity. Studies in GF CA-MLCK mice showed that commensal bacteria are required for both $CD4^+$ LP T-cell expansion and early protection against bacterial invasion. Finally, after adoptive transfer to T and B cell–deficient (*Rag1* KO) CA-MLCK mice, increased numbers of $CD4^+$ T cells from WT mice were

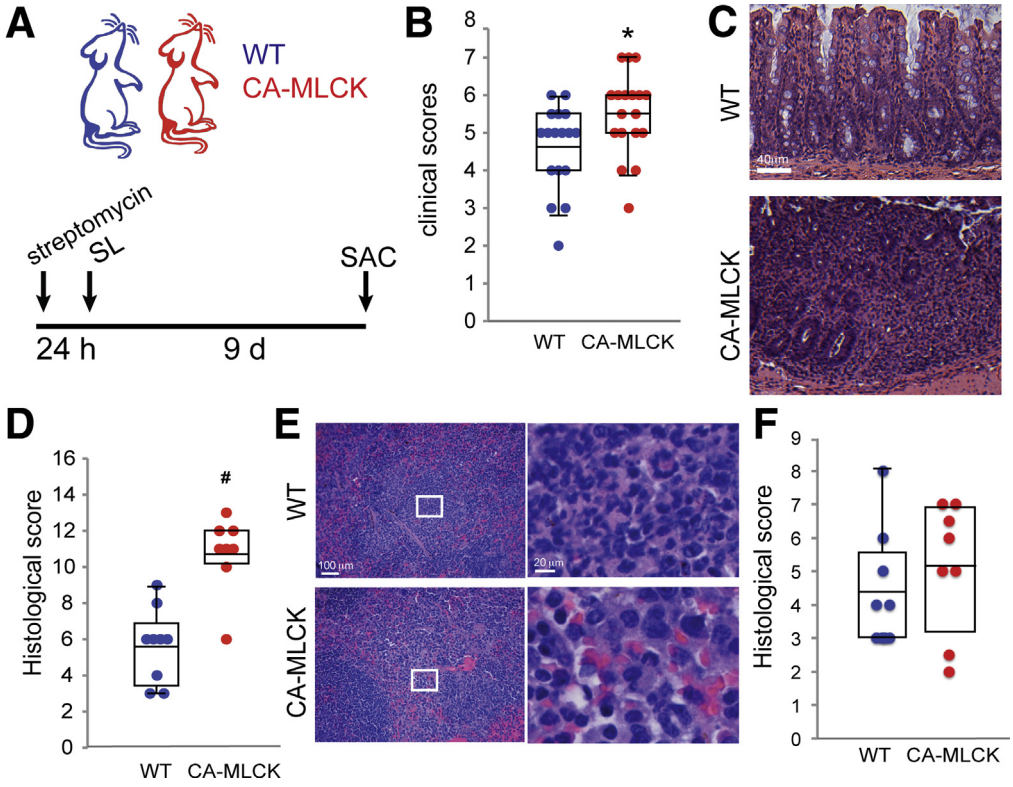

Figure 7. Constitutive barrier dysfunction enhances susceptibility to *Salmonella*-induced colitis. (*A*) WT and CA-MLCK gavaged with streptomycin 24 hours before oral infection with 10^8 CFU *S typhimurium*. (*B*) Clinical scores are shown. n = 17–18 mice from at least 3 independent experiments, $^*P < .05$. Hematoxylin-eosin micrographs and histologic scores of colon (*C* and *D*) and spleen (*E* and *F*) for infected mice are shown. n = 8–10 mice from at least 3 independent experiments are shown. $^{\#}P < .001$. SAC, sacrifice; SL, *S. typhimurium*, strain SL3201.

recruited to the LP of CA-MLCK mice where they contributed to enhanced protection against early bacterial translocation. Taken together, these findings demonstrate that the continuous low-level exposure of LP cells to commensal products as a result of physiologically relevant tight junction barrier loss drives a subclinical immune response that functions as a compensatory mechanism that limits invasion of bacterial and protozoan pathogens.

Careful consideration must be given to models of barrier dysfunction to better understand the effect of permeability in disease states because of the broad definition of "barrier defect" in the current literature.[1] For example, although intrarectal ethanol administration has been used to transiently disrupt barrier function,[21] the mechanism involves epithelial damage that likely enhances flux across the unrestricted pathway. Similarly, although JAM-A–deficient mice exhibit markedly increased intestinal permeability in addition to mucosal immune activation and inflammatory cell recruitment,[10,11] the cause of the barrier loss is likely multifactorial. Although claudins-10 and -15 are upregulated in JAM-A KO mice,[11] these claudins function as paracellular channels with diameters of 5–6 Å[3,39,40] and, therefore, cannot be responsible for the marked increases in large molecule flux reported in these mice. Furthermore, *in vitro* and *in vivo* studies have demonstrated that loss of JAM-A increases intestinal epithelial apoptosis and results in compensatory increases in epithelial proliferation *in vivo*.[10,11] Neither of these changes are present in CA-MLCK transgenic mice.

As expected for tight junction–specific barrier loss, the increased permeability induced by intestinal epithelial CA-MLCK expression is substantially lower than that observed in JAM-A knockout mice. However, the degree of barrier loss in CA-MLCK mice is quantitatively and qualitatively similar to the barrier defects reported in healthy first-degree relatives of Crohn's disease patients.[7,8] The subclinical immune activation exhibited in CA-MLCK mice confers a protective phenotype in response to acute exposure to *S typhimurium* or *T gondii*. It will be interesting to determine whether similar mucosal immune activation is present in the subset of healthy first-degree relatives of Crohn's disease patients who manifest barrier loss and whether this confers increased risk of developing disease.

The studies in GF mice indicate that mucosal immune priming in CA-MLCK mice is driven by the microbiota, which is supported by studies showing that SFB colonization induces IL17A production by $CD4^+$ T cells to promote neutrophil recruitment.[47] Consistent with this, colonization of GF CA-MLCK mice with SFB-deficient microbiota failed to restore the protective phenotype. In contrast, colonization with microbiota containing SFB was able to reduce *Salmonella* invasion in GF mice. Thus, although GF mice fail to develop a mature mucosal immune compartment and exhibit reduced mucus thickness,[49] it is not the absence of all microbes that abrogates the protection. Rather, it is the difference between TAC and JAX microbiota, most likely SFB, that explains CA-MLCK–induced microbial resistance. It is tempting to speculate that loss of these beneficial

commensals may also, in part, explain the association between acute enteritis-driven dysbiosis and the onset of chronic inflammatory bowel disease in a subset of patients.[37,38]

Similar to our initial observations demonstrating increased susceptibility of CA-MLCK mice to immune-mediated colitis,[9] we found that CA-MLCK expression in the intestinal epithelium resulted in more severe *Salmonella*-induced colitis after prolonged bacterial infection. This contrasts sharply with the protective phenotype exhibited in response to acute exposure to *S typhimurium* or *T gondii.* Due to the critical roles for IL17-dependent neutrophil recruitment in early protection against microbial invasion, it would be reasonable to hypothesize that although this early neutrophil influx clears bacteria to confer acute protection, sustained neutrophil recruitment leads to tissue destruction and more severe chronic disease. In the context of systemic infection, these data support the potential link between enteric infection and subsequent development of inflammatory bowel disease.[37,38]

Overall, these data indicate that increased intestinal epithelial tight junction permeability results in a shift in the symbiotic relationship between mucosal immunity and commensal microbes by increasing the frequency of sampling or the diversity of luminal antigens available to prime mucosal surveillance. This increased sampling may allow for constant modulation of tolerance to commensal bacteria and provide immediate protection to limit early pathogen invasion. Finally, the mechanisms identified here may explain both the absence of disease in relatives of Crohn's disease patients, despite barrier loss, as well as the increased disease susceptibility induced by barrier dysfunction.

References

1. Kiesler P, Fuss IJ, Strober W. Experimental models of inflammatory bowel diseases. Cell Mol Gastroenterol Hepatol 2015;1:154–170.
2. Ohland CL, Jobin C. Microbial activities and intestinal homeostasis: a delicate balance between health and disease. Cell Mol Gastroenterol Hepatol 2015;1:28–40.
3. Turner JR. Intestinal mucosal barrier function in health and disease. Nat Rev Immunol 2009;9:799–809.
4. Jostins L, Ripke S, Weersma RK, Duerr RH, McGovern DP, Hui KY, Lee JC, Schumm LP, Sharma Y, Anderson CA, Essers J, Mitrovic M, Ning K, Cleynen I, Theatre E, Spain SL, Raychaudhuri S, Goyette P, Wei Z, Abraham C, Achkar JP, Ahmad T, Amininejad L, Ananthakrishnan AN, Andersen V, Andrews JM, Baidoo L, Balschun T, Bampton PA, Bitton A, Boucher G, Brand S, Buning C, Cohain A, Cichon S, D'Amato M, De Jong D, Devaney KL, Dubinsky M, Edwards C, Ellinghaus D, Ferguson LR, Franchimont D, Fransen K, Gearry R, Georges M, Gieger C, Glas J, Haritunians T, Hart A, Hawkey C, Hedl M, Hu X, Karlsen TH, Kupcinskas L, Kugathasan S, Latiano A, Laukens D, Lawrance IC, Lees CW, Louis E, Mahy G, Mansfield J, Morgan AR, Mowat C, Newman W, Palmieri O, Ponsioen CY, Potocnik U, Prescott NJ, Regueiro M, Rotter JI, Russell RK, Sanderson JD, Sans M, Satsangi J, Schreiber S, Simms LA, Sventoraityte J, Targan SR, Taylor KD, Tremelling M, Verspaget HW, De Vos M, Wijmenga C, Wilson DC, Winkelmann J, Xavier RJ, Zeissig S, Zhang B, Zhang CK, Zhao H, International IBDGCSilverberg MS, Annese V, Hakonarson H, Brant SR, Radford-Smith G, Mathew CG, Rioux JD, Schadt EE, Daly MJ, Franke A, Parkes M, Vermeire S, Barrett JC, Cho JH. Host-microbe interactions have shaped the genetic architecture of inflammatory bowel disease. Nature 2012;491:119–124.
5. D'Inca R, Di Leo V, Corrao G, Martines D, D'Odorico A, Mestriner C, Venturi C, Longo G, Sturniolo GC. Intestinal permeability test as a predictor of clinical course in Crohn's disease. Am J Gastroenterol 1999;94:2956–2960.
6. Wyatt J, Vogelsang H, Hubl W, Waldhoer T, Lochs H. Intestinal permeability and the prediction of relapse in Crohn's disease. Lancet 1993;341:1437–1439.
7. Hollander D, Vadheim CM, Brettholz E, Petersen GM, Delahunty T, Rotter JI. Increased intestinal permeability in patients with Crohn's disease and their relatives: a possible etiologic factor. Ann Intern Med 1986;105:883–885.
8. Buhner S, Buning C, Genschel J, Kling K, Herrmann D, Dignass A, Kuechler I, Krueger S, Schmidt HH, Lochs H. Genetic basis for increased intestinal permeability in families with Crohn's disease: role of CARD15 3020insC mutation? Gut 2006;55:342–347.
9. Su L, Shen L, Clayburgh DR, Nalle SC, Sullivan EA, Meddings JB, Abraham C, Turner JR. Targeted epithelial tight junction dysfunction causes immune activation and contributes to development of experimental colitis. Gastroenterology 2009;136:551–563.
10. Vetrano S, Rescigno M, Cera MR, Correale C, Rumio C, Doni A, Fantini M, Sturm A, Borroni E, Repici A, Locati M, Malesci A, Dejana E, Danese S. Unique role of junctional adhesion molecule-a in maintaining mucosal homeostasis in inflammatory bowel disease. Gastroenterology 2008;135:173–184.
11. Laukoetter MG, Nava P, Lee WY, Severson EA, Capaldo CT, Babbin BA, Williams IR, Koval M, Peatman E, Campbell JA, Dermody TS, Nusrat A, Parkos CA. JAM-A regulates permeability and inflammation in the intestine in vivo. J Exp Med 2007;204:3067–3076.
12. Nalle SC, Kwak HA, Edelblum KL, Joseph NE, Singh G, Khramtsova GF, Mortenson ED, Savage PA, Turner JR. Recipient NK cell inactivation and intestinal barrier loss are required for MHC-matched graft-versus-host disease. Sci Transl Med 2014;6:243ra87.
13. Gerlach K, McKenzie AN, Neurath MF, Weigmann B. IL-9 regulates intestinal barrier function in experimental T cell-mediated colitis. Tissue Barriers 2015;3:e983777.
14. Shen L, Black ED, Witkowski ED, Lencer WI, Guerriero V, Schneeberger EE, Turner JR. Myosin light chain phosphorylation regulates barrier function by remodeling tight junction structure. J Cell Sci 2006;119:2095–2106.
15. Clayburgh DR, Barrett TA, Tang Y, Meddings JB, Van Eldik LJ, Watterson DM, Clarke LL, Mrsny RJ, Turner JR. Epithelial myosin light chain kinase-dependent barrier

dysfunction mediates T cell activation-induced diarrhea in vivo. J Clin Invest 2005;115:2702–2715.
16. Turner JR, Rill BK, Carlson SL, Carnes D, Kerner R, Mrsny RJ, Madara JL. Physiological regulation of epithelial tight junctions is associated with myosin light-chain phosphorylation. Am J Physiol 1997;273: C1378–C1385.
17. Shih VF, Cox J, Kljavin NM, Dengler HS, Reichelt M, Kumar P, Rangell L, Kolls JK, Diehl L, Ouyang W, Ghilardi N. Homeostatic IL-23 receptor signaling limits Th17 response through IL-22-mediated containment of commensal microbiota. Proc Natl Acad Sci U S A 2014; 111:13942–13947.
18. Ivanov II, Frutos Rde L, Manel N, Yoshinaga K, Rifkin DB, Sartor RB, Finlay BB, Littman DR. Specific microbiota direct the differentiation of IL-17-producing T-helper cells in the mucosa of the small intestine. Cell Host Microbe 2008;4:337–349.
19. Hooper LV, Littman DR, Macpherson AJ. Interactions between the microbiota and the immune system. Science 2012;336:1268–1273.
20. Cao AT, Yao S, Gong B, Elson CO, Cong Y. Th17 cells upregulate polymeric Ig receptor and intestinal IgA and contribute to intestinal homeostasis. J Immunol 2012; 189:4666–4673.
21. Boirivant M, Amendola A, Butera A, Sanchez M, Xu L, Marinaro M, Kitani A, Di Giacinto C, Strober W, Fuss IJ. A transient breach in the epithelial barrier leads to regulatory T-cell generation and resistance to experimental colitis. Gastroenterology 2008;135:1612–1623 e5.
22. Khounlotham M, Kim W, Peatman E, Nava P, Medina-Contreras O, Addis C, Koch S, Fournier B, Nusrat A, Denning TL, Parkos CA. Compromised intestinal epithelial barrier induces adaptive immune compensation that protects from colitis. Immunity 2012;37:563–573.
23. Weber CR, Raleigh DR, Su L, Shen L, Sullivan EA, Wang Y, Turner JR. Epithelial myosin light chain kinase activation induces mucosal interleukin-13 expression to alter tight junction ion selectivity. J Biol Chem 2010; 285:12037–12046.
24. Prinz I, Sansoni A, Kissenpfennig A, Ardouin L, Malissen M, Malissen B. Visualization of the earliest steps of gammadelta T cell development in the adult thymus. Nat Immunol 2006;7:995–1003.
25. Yang H, Madison B, Gumucio DL, Teitelbaum DH. Specific overexpression of IL-7 in the intestinal mucosa: the role in intestinal intraepithelial lymphocyte development. Am J Physiol Gastrointest Liver Physiol 2008; 294:G1421–G1430.
26. Harriman GR, Bogue M, Rogers P, Finegold M, Pacheco S, Bradley A, Zhang Y, Mbawuike IN. Targeted deletion of the IgA constant region in mice leads to IgA deficiency with alterations in expression of other Ig isotypes. J Immunol 1999;162:2521–2529.
27. Marchiando AM, Shen L, Graham WV, Weber CR, Schwarz BT, Austin JR 2nd, Raleigh DR, Guan Y, Watson AJ, Montrose MH, Turner JR. Caveolin-1-dependent occludin endocytosis is required for TNF-induced tight junction regulation in vivo. J Cell Biol 2010;189:111–126.
28. Edelblum KL, Singh G, Odenwald MA, Lingaraju A, El Bissati K, McLeod R, Sperling AI, Turner JR. Gammadelta intraepithelial lymphocyte migration limits transepithelial pathogen invasion and systemic disease in mice. Gastroenterology 2015;148:1417–1426.
29. Cong H, Mui EJ, Witola WH, Sidney J, Alexander J, Sette A, Maewal A, El Bissati K, Zhou Y, Suzuki Y, Lee D, Woods S, Sommerville C, Henriquez FL, Roberts CW, McLeod R. Toxoplasma gondii HLA-B*0702-restricted GRA7(20-28) peptide with adjuvants and a universal helper T cell epitope elicits CD8(+) T cells producing interferon-gamma and reduces parasite burden in HLA-B*0702 mice. Hum Immunol 2012;73:1–10.
30. Hutson SL, Mui E, Kinsley K, Witola WH, Behnke MS, El Bissati K, Muench SP, Rohrman B, Liu SR, Wollmann R, Ogata Y, Sarkeshik A, Yates JR 3rd, McLeod R. T. gondii RP promoters & knockdown reveal molecular pathways associated with proliferation and cell-cycle arrest. PLoS One 2010;5:e14057.
31. Edelblum KL, Shen L, Weber CR, Marchiando AM, Clay BS, Wang Y, Prinz I, Malissen B, Sperling AI, Turner JR. Dynamic migration of gammadelta intraepithelial lymphocytes requires occludin. Proc Natl Acad Sci U S A 2012;109:7097–7102.
32. Al-Anouti F, Tomavo S, Parmley S, Ananvoranich S. The expression of lactate dehydrogenase is important for the cell cycle of Toxoplasma gondii. J Biol Chem 2004; 279:52300–52311.
33. Lindner C, Wahl B, Fohse L, Suerbaum S, Macpherson AJ, Prinz I, Pabst O. Age, microbiota, and T cells shape diverse individual IgA repertoires in the intestine. J Exp Med 2012;209:365–377.
34. Lindner C, Thomsen I, Wahl B, Ugur M, Sethi MK, Friedrichsen M, Smoczek A, Ott S, Baumann U, Suerbaum S, Schreiber S, Bleich A, Gaboriau-Routhiau V, Cerf-Bensussan N, Hazanov H, Mehr R, Boysen P, Rosenstiel P, Pabst O. Diversification of memory B cells drives the continuous adaptation of secretory antibodies to gut microbiota. Nat Immunol 2015;16:880–888.
35. Brochet X, Lefranc MP, Giudicelli V. IMGT/V-QUEST: the highly customized and integrated system for IG and TR standardized V-J and V-D-J sequence analysis. Nucleic Acids Res 2008;36:W503–W508.
36. Lefranc MP, Giudicelli V, Ginestoux C, Jabado-Michaloud J, Folch G, Bellahcene F, Wu Y, Gemrot E, Brochet X, Lane J, Regnier L, Ehrenmann F, Lefranc G, Duroux P. IMGT, the international ImMunoGeneTics information system. Nucleic Acids Res 2009; 37:D1006–D1012.
37. Gradel KO, Nielsen HL, Schonheyder HC, Ejlertsen T, Kristensen B, Nielsen H. Increased short- and long-term risk of inflammatory bowel disease after salmonella or campylobacter gastroenteritis. Gastroenterology 2009; 137:495–501.
38. Garcia Rodriguez LA, Ruigomez A, Panes J. Acute gastroenteritis is followed by an increased risk of inflammatory bowel disease. Gastroenterology 2006; 130:1588–1594.
39. Nalle SC, Turner JR. Intestinal barrier loss as a critical pathogenic link between inflammatory bowel disease

and graft-versus-host disease. Mucosal Immunol 2015; 8:720–730.
40. Anderson JM, Van Itallie CM. Physiology and function of the tight junction. Cold Spring Harb Perspect Biol 2009; 1:a002584.
41. Ismail AS, Severson KM, Vaishnava S, Behrendt CL, Yu X, Benjamin JL, Ruhn KA, Hou B, DeFranco AL, Yarovinsky F, Hooper LV. Gammadelta intraepithelial lymphocytes are essential mediators of host-microbial homeostasis at the intestinal mucosal surface. Proc Natl Acad Sci U S A 2011;108:8743–8748.
42. Fagarasan S, Kawamoto S, Kanagawa O, Suzuki K. Adaptive immune regulation in the gut: T cell-dependent and T cell-independent IgA synthesis. Annu Rev Immunol 2010;28:243–273.
43. Goto Y, Obata T, Kunisawa J, Sato S, Ivanov II, Lamichhane A, Takeyama N, Kamioka M, Sakamoto M, Matsuki T, Setoyama H, Imaoka A, Uematsu S, Akira S, Domino SE, Kulig P, Becher B, Renauld JC, Sasakawa C, Umesaki Y, Benno Y, Kiyono H. Innate lymphoid cells regulate intestinal epithelial cell glycosylation. Science 2014;345:1254009.
44. Ouyang W, Kolls JK, Zheng Y. The biological functions of T helper 17 cell effector cytokines in inflammation. Immunity 2008;28:454–467.
45. Geddes K, Rubino SJ, Magalhaes JG, Streutker C, Le Bourhis L, Cho JH, Robertson SJ, Kim CJ, Kaul R, Philpott DJ, Girardin SE. Identification of an innate T helper type 17 response to intestinal bacterial pathogens. Nat Med 2011;17:837–844.
46. Fossiez F, Djossou O, Chomarat P, Flores-Romo L, Ait-Yahia S, Maat C, Pin JJ, Garrone P, Garcia E, Saeland S, Blanchard D, Gaillard C, Das Mahapatra B, Rouvier E, Golstein P, Banchereau J, Lebecque S. T cell interleukin-17 induces stromal cells to produce proinflammatory and hematopoietic cytokines. J Exp Med 1996;183:2593–2603.
47. Flannigan KL, Ngo VL, Geem D, Harusato A, Hirota SA, Parkos CA, Lukacs NW, Nusrat A, Gaboriau-Routhiau V, Cerf-Bensussan N, Gewirtz AT, Denning TL. IL-17A-mediated neutrophil recruitment limits expansion of segmented filamentous bacteria. Mucosal Immunol 2017;10:673–684.
48. Ivanov II, Atarashi K, Manel N, Brodie EL, Shima T, Karaoz U, Wei D, Goldfarb KC, Santee CA, Lynch SV, Tanoue T, Imaoka A, Itoh K, Takeda K, Umesaki Y, Honda K, Littman DR. Induction of intestinal Th17 cells by segmented filamentous bacteria. Cell 2009;139: 485–498.
49. Johansson ME, Jakobsson HE, Holmen-Larsson J, Schutte A, Ermund A, Rodriguez-Pineiro AM, Arike L, Wising C, Svensson F, Backhed F, Hansson GC. Normalization of host intestinal mucus layers requires long-term microbial colonization. Cell Host Microbe 2015;18:582–592.

Received February 22, 2017. Accepted June 5, 2017.

Correspondence
Address correspondence to: Karen L. Edelblum, PhD, Rutgers New Jersey Medical School, 205 South Orange Avenue, Cancer Center G1228, Newark, New Jersey 07103. e-mail: ke163@njms.rutgers.edu; or Jerrold R. Turner, MD, PhD, Brigham and Women's Hospital, 20 Shattuck Street, Thorn 1428, Boston, Massachusetts 02115. e-mail: jrturner@bwh.harvard.edu.

Acknowledgments
The authors thank Sara McBride for help with mouse rederivation, Taren Thorn and Kimberly Ly for animal care, and the Frank W. Fitch Monoclonal Antibody Core Facility at the University of Chicago for monoclonal antibody production.

Author contributions
Conceptualization, K.L.E and J.R.T.; methodology, K.L.E., G. Sharon, and S.K.M.; formal analysis, S.R. and I.T.; investigation, K.L.E., G. Sharon, G. Singh, A.S., S.C., S.G., S.R., K.E.B., and J.R.T.; resources, S.K.M., R.M., C.D., I.P., and J.R.T.; writing-original draft, K.L.E.; writing-review and editing, K.L.E., G. Sharon, S.K.M., R.M., K.E.B., I.P., S.R., and J.R.T.; visualization, K.L.E., S.R, and I.P.; supervision, K.L.E., S.K.M., and J.R.T.; funding, K.L.E., S.K.M., and J.R.T.

Conflicts of interest
The authors disclose no conflicts.

One author (J.R.T.) is a member of the CMGH Board of Editors (BOE). In accordance with journal policy, the review process for this manuscript was managed by a Guest Associate Editor, and the author BOE member was blinded to the entire process.

Funding
Supported by National Institute of Health grants K01DK093627 and F32DK084859 (K.L.E.), R01DK078938, R01GM099535 (S.K.M.), R01DK61931 and R01DK68271 (J.R.T.); Department of Defense W81XWH-09-1-0341 (J.R.T.); Crohn's and Colitis Foundation of America (S.K.M. and J.R.T.) and Broad Medical Research Foundation (J.R.T.); The Human Frontiers Science Program - Long Term Fellowship (G. Sharon); and the Heritage Medical Research Institute (S.K.M.)